Available online at www.sciencedirect.com
ScienceDirect
Ceramics International 37 (2011) 1085–1092
CERAMICS INTERNATIONAL
www.elsevier.com/locate/ceramint

Reaction sintering of colloidal processed mixtures of sub-micrometric alumina and nano-titania

M.I. Nieto [a], C. Baudín [a], I. Santacruz [b,*]

[a] Instituto de Cerámica y Vidrio, CSIC, Kelsen 5, 28049 Madrid, Spain
[b] Departamento de Química Inorgánica, Cristalografía y Mineralogía, Universidad de Málaga, 29071 Málaga, Spain

Received 29 September 2010; received in revised form 17 October 2010; accepted 17 November 2010
Available online 25 December 2010

Abstract

The fabrication of composites formed by alumina grains (95 vol%) in the micrometer size range and aluminium titanate nanoparticles (5 vol%) by reaction sintering of alumina (Al_2O_3) and titania (TiO_2) is investigated. The green bodies were constituted by mixtures of sub-micrometric alumina and nano-titania obtained from freeze-drying homogeneous water based suspensions, and pressing the powders. The optimization of the colloidal processing variables was performed using the viscosity of the suspensions as control parameter. Different one step and two step sintering schedules using as maximum dwell temperatures 1300 and 1400 °C were established from dynamic sintering experiments. Specimens cooled at 5 °C/min as well as quenched specimens were prepared and characterized in terms of crystalline phases, by X-ray diffraction, and microstructure by scanning electron microscopy of fracture surfaces.

Even though homogeneous final materials were obtained in all cases, full reaction was obtained only in materials treated at 1400 °C. The microstructure of the composites obtained by quenching was formed by an alumina matrix with bimodal grain size distribution and submicrometric aluminium titanate grains located inside the largest alumina grains and at triple points. However a cooling rate of 5 °C/min led to significant decomposition of aluminium titanate. This fact is attributed to the small size of the particles and the effect of the alumina surrounding matrix.

Keywords: A. Suspensions; B. Nanocomposites; D. Al_2O_3; D. Al_2TiO_5

1. Introduction

Dense and fine grained alumina (Al_2O_3) materials have attractive properties such as wear and deformation resistance and chemical inertness, but they lack toughness and flaw tolerance and, consequently they present poor associated behavioural properties such as thermal shock resistance.

From the different second phases that have been proposed to improve the mechanical behaviour of alumina materials, aluminium titanate (Al_2TiO_5) is one of the most attractive because it is compatible with alumina and alumina–aluminium titanate composites can present a wide range of properties as a function of the microstructure. Thermal expansion of aluminium titanate is highly anisotropic ($\alpha_{a25-1000\,^\circ C} = 10.9 \times 10^{-6}\,^\circ C^{-1}$, $\alpha_{b25-1000\,^\circ C} = 20.5 \times 10^{-6}\,^\circ C^{-1}$, $\alpha_{c25-1000\,^\circ C} = -2.7 \times 10^{-6}\,^\circ C^{-1}$)[1] [1] and alumina shows limited anisotropy ($\alpha_{a25-1000\,^\circ C} = 8.4 \times 10^{-6}\,^\circ C^{-1}$, $\alpha_{c25-1000\,^\circ C} = 9.2 \times 10^{-6}\,^\circ C^{-1}$) [2]. Therefore, tensile or compressive residual stresses, function of the particular crystallographic orientation of the grains, develop in the sintered materials. Depending on the material composition, the grain sizes and the characteristics of the grain boundaries, microcracking might occur during cooling from sintering and/or during fracture. The adequate manipulation of the level of these stresses via microstructural design in monolithic and layered materials can lead to materials with improved flaw tolerance and/or toughness [3–14].

Alumina–aluminium titanate monolithic composites showing R-curve behaviour were reported in the 1990s [3–6]. Those materials had aluminium titanate contents 20–30 vol% and

* Corresponding author. Tel.: +34 952 132022; fax: +34 952 131870.
E-mail address: isantacruz@uma.es (I. Santacruz).

[1] In this work, β-Al_2TiO_5 orthorhombic crystal is described by a b-face centered unit cell, space group Bbmm, $a = 9.439$ Å, $b = 9.647$ Å, $c = 3.593$ Å.

0272-8842/$36.00
doi:10.1016/j.ceramint.2010.11.030

presented different levels of microcracks in the "as sintered" state. Crack bridging by second phase agglomerates and by large alumina grains was identified as the toughening mechanism. A later work showed that both second phase and matrix grains could act as bridges in the wake of the propagating crack in a microcrack free and fine grained alumina + 10 vol% aluminium titanate composite prepared from alumina and aluminium titanate mixtures [7]. Such material presented increased thermal shock resistance compared to a monophase alumina of similar grain size while maintaining strength. The microstructure of alumina + 10 vol% aluminium titanate composites obtained by reaction sintering of alumina and titania (TiO_2) presented special features that led to extensive microcracking as the main toughening mechanism [12]. In such material microcracking was partially due to the presence of nanometric second phase particles at the grain boundaries between the alumina grains, which led to intergranular fracture.

Aluminium titanate is the only stable compound in the alumina–titania system above 1280 °C up to its melting point. Below that temperature it would decompose to produce α-Al_2O_3 and TiO_2 (rutile). Decomposition is not favourable kinetically under 900 °C and maximum rates reported occur at about 1100 °C. In general, decomposition rates are low enough to permit the existence of aluminium titanate materials at room temperature. However, significant decomposition (~20%) of a monophase material with relative large grains (~20 μm) on cooling from the sintering temperature (10 °C/min) between 1200 and 1000 °C has been reported [15].

Initially a nucleation and growth controlled process, affected by the characteristics of the microstructure of the material, was proposed as main decomposition mechanism [16,17]. Recent studies propose the atomic diffusion as controlling mechanism [15,18]. High-temperature studies of the β-Al_2TiO_5 crystalline structure revealed an increasing substitution of Al for the Ti atoms in the crystal in the temperature range 900–1280 °C. As signalled by Skala et al. [18], the increase in the occupancy of the Al atoms and the temperature range over which it occurred may indicate that these are "pre-transformation" or pre-eutectoid changes at the atomic scale that may enhance subsequent eutectoid decomposition on cooling.

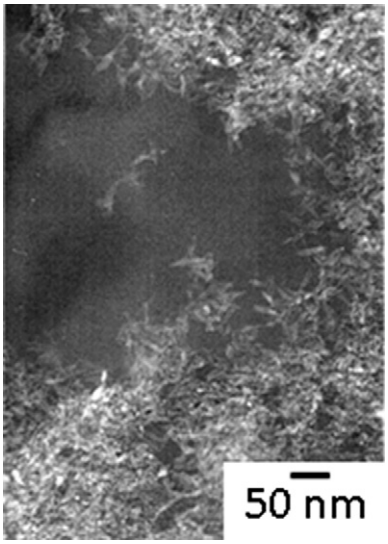

Fig. 1. TiO_2 powder obtained after drying the "as received" nanosuspension showing the needle-like shape of the particles. Transmission electron micrograph.

Another factor that has been proposed as determinant of the thermal behaviour of β-Al_2TiO_5 is the complex system of internal stresses and fractures that may develop in the material during cooling from elevated temperatures, resulting from the thermal expansion mismatch between individual grains [13,18,19]. Aluminium titanate formation is expansive and, therefore, particles under a compressive stresses will be more prone to decomposition.

Segadaes et al. [16] proposed that residual alumina particles might act as preferred nucleation sites for the decomposition of β-Al_2TiO_5 in alumina–aluminium titanate composites.

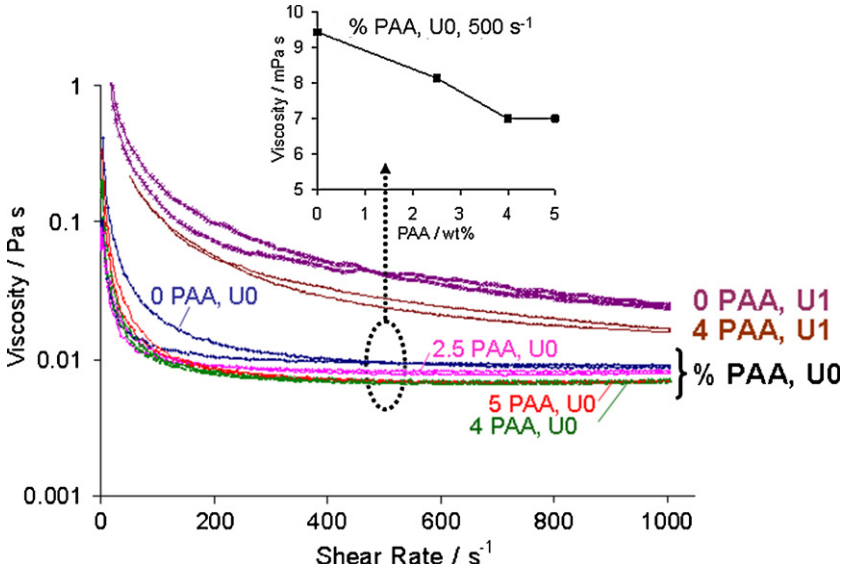

Fig. 2. Viscosity curves for titania suspensions with different deflocculant (PAA) contents prepared with (U1) and without ultrasonication (U0). The inset figure shows the viscosity of the U0 suspensions as a function of the PAA content at a shear rate of 500 s^{-1}.

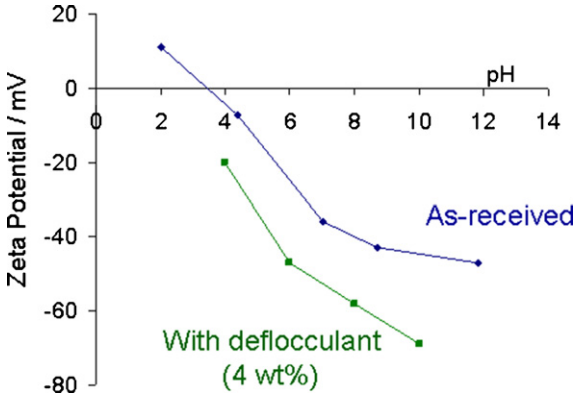

Fig. 3. Zeta potential values vs. pH of the as received (w/o PAA) and 4 wt%-deflocculated titania suspensions.

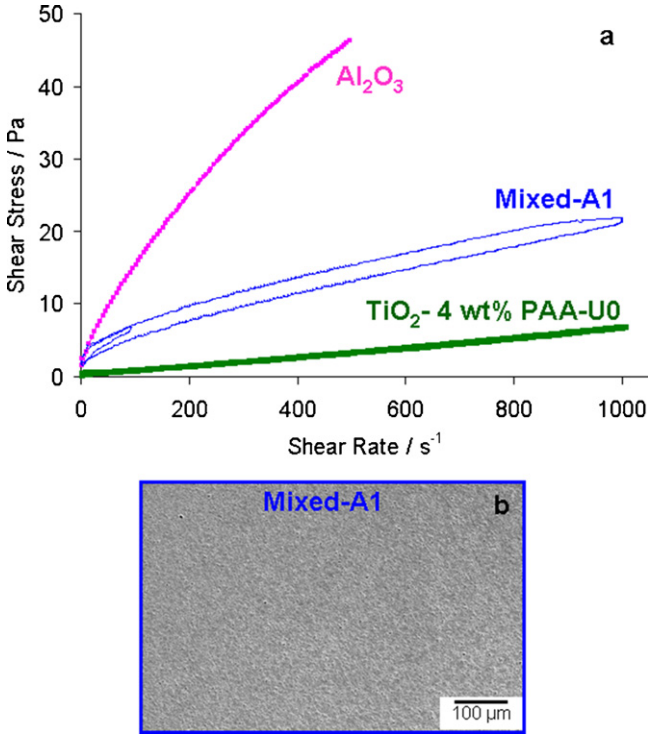

Fig. 4. Flow curves of the optimized 80 wt%-alumina, 8 wt%-titania suspensions and mixed suspensions after 1 h attrition milling (a), and FEG-SEM micrograph of the milled sample obtained from mixed suspensions after sintering at 1400 °C/1 h (b).

Furthermore, the changes in the atomic scale proposed by Skala et al. [18] as responsible for decomposition will be favoured in materials with alumina excess. Moreover, the thermal expansion mismatch between alumina and aluminium titanate could also contribute to the decomposition because the crystalline average thermal expansion of aluminium titanate ($\sim 10 \times 10^{-6}\,^{\circ}C^{-1}$) is higher than that of alumina ($\sim 8 \times 10^{-6}\,^{\circ}C^{-1}$).

However, no experimental evidence of increased β-Al_2TiO_5 instability in alumina–aluminium titanate composites has been reported. In particular, different authors have reported fine grained (grain size < 2.2 μm and $d_{50} \sim 0.8$ μm [7,14] and grain size $d_{50} \sim 1.5$ μm [20]) dense and uncracked composite materials with 5–20 vol% of aluminium titanate and porous materials with 30 vol% of aluminium titanate processed from nanostructured alumina–titania aggregates [21] have been reported.

In this work, the fabrication of composites formed by alumina grains (95 vol%) in the micrometer size range and aluminium titanate nanoparticles (5 vol%) is investigated. The initial objective pursued with such materials was to analyze the effect of the residual stresses in composites with grain sizes far from the critical ones for microcracking. It was our hypothesis

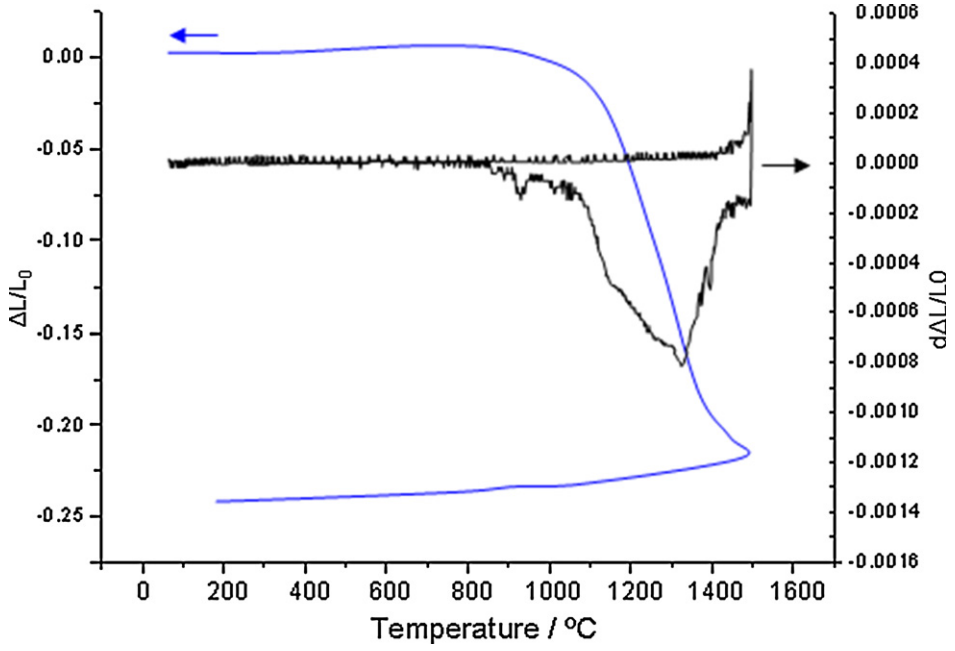

Fig. 5. Dynamic sintering curves (heating and cooling) of the optimized green material (mixed suspension after 1 h milling).

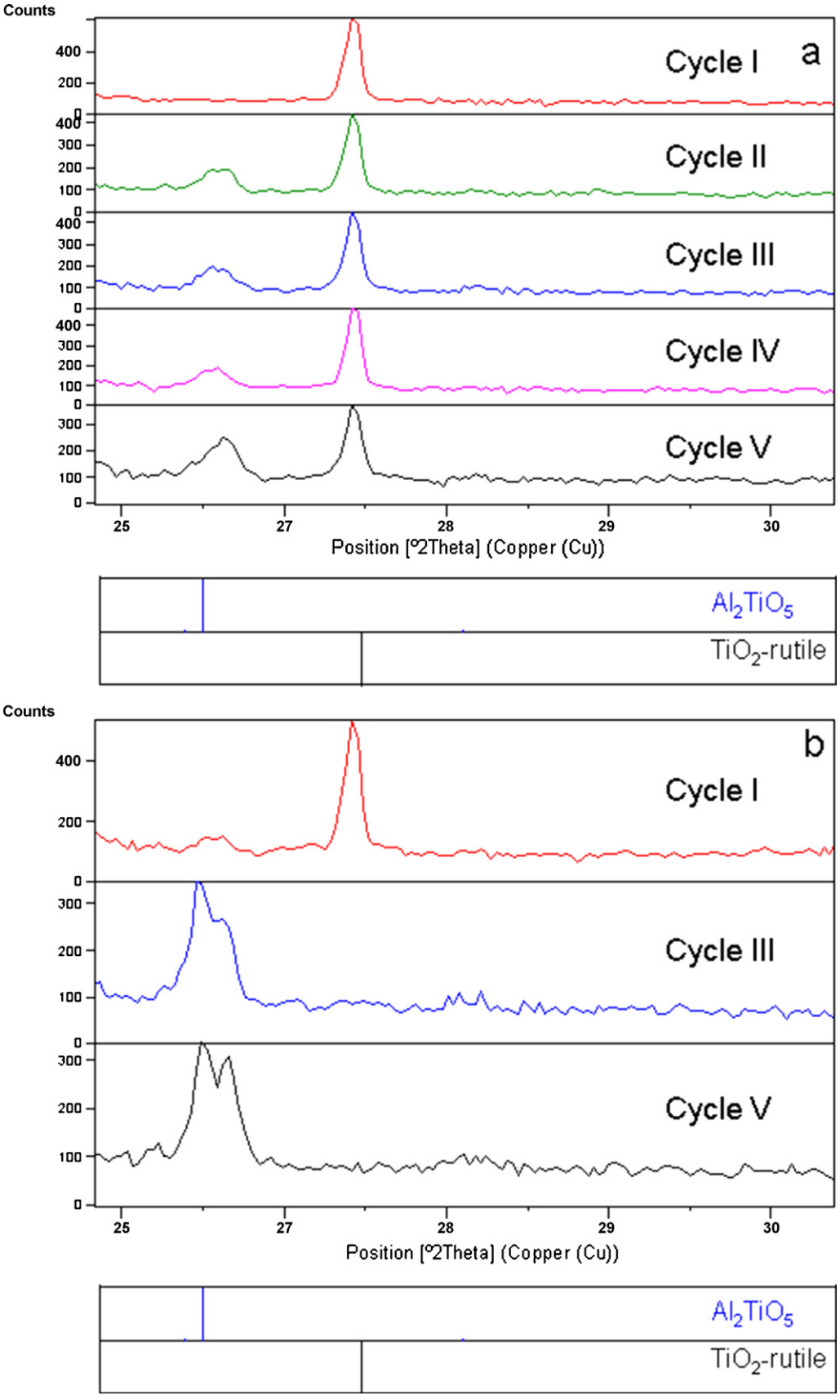

Fig. 6. X-ray diffraction of sintered samples cooled at 5 °C/min (a) and quenched (b).

that decreasing the size of the second phase particles and the total amount of aluminium titanate would improve the strength of the material. However, it has not been possible to obtain fully reacted composites using standard cooling rates after sintering.

The green bodies were fabricated from homogeneously dispersed suspensions of submicrometer alumina and nanometric titania in order to assure the isolation of the aluminium titanate particles in the alumina matrix and, thus, to avoid their growth. As the commercial nanopowders are usually agglomerated, a commercial suspension was used as starting titania. The direct use of commercial nanosuspensions has been demonstrated to be an advance [22].

2. Experimental

Alumina and titania mixtures in proportion to obtain alumina + 5 vol% aluminium titanate composites by reaction sintering were used to prepare the green bodies. Commercial α-Al_2O_3 was used (Condea HPA05, USA) with a mean particle size of 0.35 μm and a specific surface area of 9.5 m^2/g. Aqueous alumina suspensions were prepared to solids loadings of 83 wt% (55 vol%) by ball milling for 6 h with alumina jar and balls. An ammonium salt of polyacrylic acid, PAA, (Duramax D3005, Rohm & Haas, USA) with an average molecular weight of ~2400 Da and a 35 wt% active matter, was used as deflocculant at a fixed concentration of 0.8 wt% of active matter on a dry solids basis, according to previous works [12,23]. The resulting pH value was 9.0 ± 0.1. The suspensions were shacked in closed flasks for 24 h in order to reach an adequate surface equilibrium.

The titania precursor was a commercial nanosuspension (S311, TPL, China) that contained 8 wt% titania nanoparticles (TiO_2) in deionised water with organic additives. This solid loading was determined by drying the suspension in an oven at 60 °C overnight and subsequent thermogravimetric analysis (TGA, Netzsch STAY09, Germany). This nanosized powder was characterized by transmission electron microscopy, TEM (JEOL 2000FX, Jeol, Tokyo, Japan). The phase present in this powder was determined by X-ray diffraction (Siemens AG, D5000, Germany) and the result was processed using the anatase ASTM File [24]. The effect of the same anionic dispersant as the one used to prepare the alumina suspensions on the rheological behaviour of the commercial titania one was examined. Deflocculant amounts in the range 0–5 wt% of active matter on a dry solids basis were used. The effect of ultrasound (U) on this suspension without and with PAA was studied using a 400 W sonication probe (UP400s Hielscher Ultrasonics GmbH, Stuttgart, Germany).

The rheological measurements were performed using a rheometer (Model RS50, Thermo Haake, Karlsruhe, Germany) with a double-cone and plate system (60 mm in diameter, 2° cone angle) with a solvent trap to reduce evaporation. A three-stage measuring program with a linear increase in the shear rate from 0 to 1000 s^{-1} in 300 s, a plateau at 1000 s^{-1} for 120 s, and a further decrease to zero shear rate in 300 s was used. The zeta potential was measured on dilute aqueous titania suspensions,

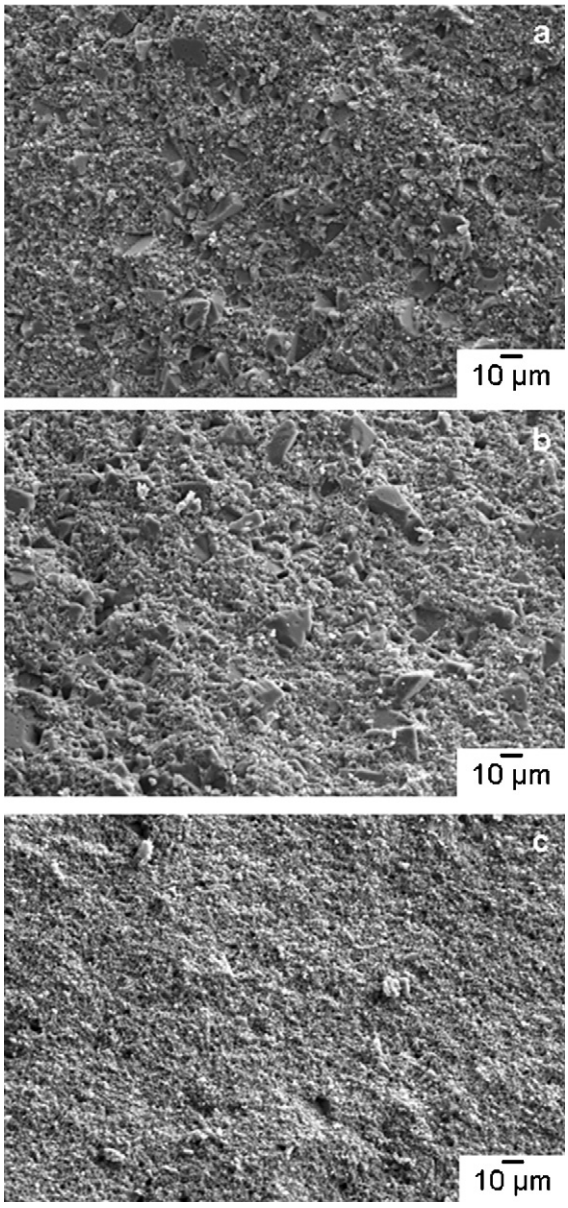

Fig. 7. Fracture surfaces of samples sintered using cycles III-5 °C/min cooling (a), III-quenching (b) and I-quenching (c).

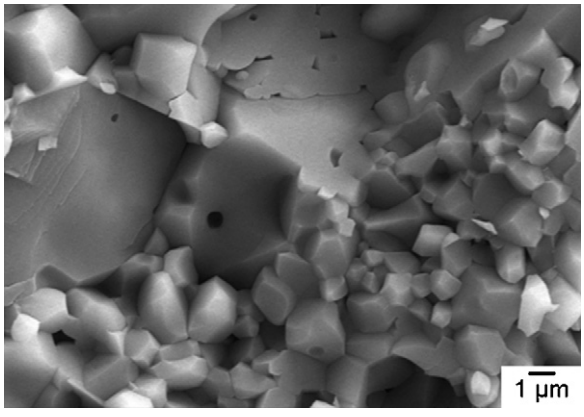

Fig. 8. SEM microstructure of the fracture surface of the quenched sample sintered using cycle III at higher magnification.

1.0 wt% solids content, with (4 wt%) and without dispersant at different pH, by dynamic light scattering (Zetasizer NanoZS, Malvern Instruments, Malvern, UK).

Mixed suspensions with a final solids loading of 72 wt% were prepared by the combination of both optimized suspensions in the ratio required to achieve a 5 vol% Al_2TiO_5 in the Al_2O_3 matrix after reaction sintering. Homogenization was performed in an attrition mill with alumina balls for 1 h. Then the suspension was divided into different flasks and frozen by immersing the flasks in liquid nitrogen and rotating them. The frozen mixture was freeze dried for 48 h (CRYODOS-50, Telstar, Spain), sieved through a 100 μm mesh and isostatically pressed (200 MPa, National Forge Europe, Belgium). The densities of the green bodies were measured using the Archimedes' method in mercury. Theoretical densities were calculated taking values of 3.99 g cm^{-3} for alumina [25], and 3.89 g cm^{-3} for anatase [24].

Dynamic sintering studies were performed with a differential dilatometer (Setsys 16/18, Setaram, France) in air up to 1500 °C in order to select the adequate isothermal sintering treatments. Different one and two-step sintering cycles were established as a function of the formation temperature of aluminium titanate and the shrinkage temperatures established from the dynamic sintering experiments. The following sintering cycles were analyzed: 1300 °C/1 h (Cycle I), 1400 °C/1 h (Cycle II), 1150 °C/1 h–1400 °C/1 h (Cycle III), 1300 °C/10 h (Cycle IV), 1400 °C/0 h–1300 °C/10 h (Cycle V). The heating and cooling rates were 5 °C/min. For selected cycles, quenched specimens were also fabricated by extracting the specimens from the furnace at the sintering temperature and cooling them in an air stream. The densities of the sintered bodies were measured using the Archimedes' method in water.

All sintered compounds were characterized by high resolution laboratory X-ray powder diffraction (LXRPD) at room temperature. Powder patterns were collected on a Philips X'Pert Pro MPD automated diffractometer equipped with a Ge(1 1 1) primary monochromator (strictly monochromatic $CuK_{\alpha 1}$ radiation) and an X'Celerator detector (PANalytical B.V., Almelo, Netherlands). The overall measurement time was ~4 h per pattern to have good statistics over the 2θ range of 20–80° with a 0.017° step size, and analyses were carried out on using the structural description reported previously for Al_2O_3 [25], TiO_2-rutile [26] and Al_2TiO_5 [27].

Microstructural characterization was performed by field emission gun scanning electron microscopy, FEG-SEM (JEOL 2010F, Tokyo, Japan), on fracture surfaces.

3. Results and discussion

Fig. 1 shows a TEM micrograph of the titania powder obtained after drying the "as received" nanosuspension. Those particles have needle shape, diameters of few nanometres and lengths shorter than 50 nm. XRD showed that they were in the anatase phase. TG/TDA experiments indicated that the dried powder contained 5 wt% of water and a high amount of binders, 17 wt%, to be considered for calculations.

Fig. 2 shows the viscosity curves for titania suspensions with different PAA contents (wt%) prepared with 1 min (U1) and without ultrasonication (U0). From the suspensions prepared without sonication, the one with a concentration of 4 wt% PAA shows slightly lower viscosity values at all shear rates than the others. This fact is better illustrated in the inset, where the deflocculation curve for a shear rate of 500 s^{-1} is shown; a minimum viscosity of 7 MPa s was obtained. Ultrasonication led to higher viscosity at all shear rates, with a more notorious destabilization effect for the "as received" suspension. Thus, ultrasonication was rejected for further studies.

Fig. 3 shows zeta potential values vs. pH of the as received and 4 wt%-deflocculated titania suspensions. The shifting of the isoelectric point towards a more acidic value shows that the PAA was adsorbed onto the ceramic particles, despite the relatively high amount of organics (17 wt%) present in the commercial suspension. The shifting demonstrates that the polyelectrolyte provides further stabilization to the commercial suspension at the studied range of pH.

Fig. 4a shows the flow curves of the optimized mixed and monophase 80 wt%-alumina and 8 wt%-titania suspensions. The alumina suspension showed the highest viscosity values at any shear rate which can be attributed to its relatively high solids loading. Correspondingly, the optimized monophase titania suspension presented the lowest viscosity and the mixed one showed intermediate viscosity. Fig. 4b shows the characteristic microstructure of specimens prepared by slip casting of the mixed suspension and sintered at 1400 °C/1 h. No large defects are observed, therefore, the process followed to prepare alumina–titania suspensions was considered adequate for further experiments.

The density of the green samples was 57 ± 1% of the theoretical. Fig. 5 shows the dilatometric curves recorded during the dynamic sintering tests. Shrinkage starts at ~900 °C and it accelerates at ~1100 °C. Then, the shrinkage rate diminishes at ~1300 °C, until a final arrest at ~1450 °C. The decrease of the shrinkage rate is due to the expansive formation of Al_2TiO_5, as previously reported for reaction sintered alumina–10 vol% aluminium titanate composites obtained from micronsized powders [28].

Therefore, temperatures of 1300 and 1400 °C were selected for one and two step static sintering studies to assure the full reaction of the material. No higher temperatures were studied in order to limit grain growth. Two different times (1 and 10 h) were tried for the lowest temperature whereas a standard time of 1 h at 1400 °C was considered as sufficient for full reaction. The effect of two step sintering cycles was analyzed because they have been proposed and proved in the literature to be a good method for densification avoiding grain growth [29,30]. One of the two step cycles was designed with a low temperature step of 1 h at 1150 °C, to enhance densification before reaction, and a high temperature step at 1400 °C to assure full reaction. The other two step cycle was designed in order to analyze the effect of a high temperature instantaneous treatment (1400 °C – 0 h) prior to the low temperature long step (1300 °C – 10 h) which has been demonstrated to avoid grain growth in non-reacting materials [29,30]. As shown in Fig. 6a, none of the

thermal treatments performed using a standard cooling rate for ceramics (5 °C/min) led to fully reacted alumina–aluminium titanate materials and even no aluminium titanate was present in the material treated at 1300 °C during 1 h. This latter dwell temperature and time allowed very limited reaction as shown by the fact that only traces of aluminium titanate were detected in the quenched material (Fig. 6b). However, fully reacted materials were obtained after both two step treatments when quenching was used (Fig. 6b). These results confirm that aluminium titanate is obtained by reaction sintering of alumina and titania at temperatures between 1300 and 1400 °C, according to previous results for micron-sized materials [20,31]. However, no decomposition of aluminium titanate was reported in those reaction sintered materials [20,31] or in materials fabricated from aluminium titanate (5–10 vol%) and alumina mixtures with aluminium titanate sizes between 0.5 and 2.2 μm, for which thermal treatments of 4 h at temperatures between 1000 and 1100 °C led to negligible decomposition (and full decomposition occurred only for higher temperatures (1200–1250 °C)) [7,14].

Low magnification micrographs of fracture surfaces of selected materials are collected in Fig. 7. All materials treated at 1400 °C presented bimodal microstructures with exaggerated alumina grain growth and associated intragranular porosity (Fig. 7a and b) whereas thermal treatments at 1300 °C led to homogeneous alumina grain sizes (Fig. 7c). It is well known that titania accelerates the mass transport mechanisms in alumina and could lead to exaggerated grain growth at high temperature when small amounts of titania are present [9]. However, once the solid solubility limit of titania in alumina at the considered temperature is surpassed, the formation of aluminium titanate is a competing process that arrests grain growth. In fact, alumina–aluminium titanate materials with homogeneous microstructures have been reported [20,28,31]. Such differences have to be associated to the raw materials used to fabricate the materials studied here. As shown in Fig. 8, the microstructure of the alumina–aluminium titanate composites obtained by quenching was formed by the bimodal alumina matrix and submicrometric second phase grains located inside the large alumina grains and at triple points. The small size intragranular aluminium titanate grains were easily trapped by the alumina growing grains during sintering and no grain growth arrest occurred.

The phase development observed in the studied materials during cooling using a standard rate demonstrates the validity of the proposal by Segadaes et al. [16] concerning the role of alumina particles as nucleation sites for the decomposition of aluminium titanate. Decomposition of the small submicrometric second phase particles surrounded by alumina in the materials studied here will be greatly enhanced with respect to that of the larger ones present in other composites.

4. Conclusions

The fabrication of alumina (95 vol%) and aluminium titanate (5 vol%) nanocomposites by reaction sintering at 1300 and 1400 °C of submicrometric alumina (Al_2O_3) and nanometric titania (TiO_2) mixtures has been investigated. Full reaction was obtained only in materials treated at 1400 °C and quenched. Standard ceramic processing cooling rate (5 °C/min) led to significant decomposition of aluminium titanate due to the small size of the particles and the effect of the alumina surrounding matrix. This fact limits the possibility of improving the strength of alumina–aluminium titanate materials via the microstructural refining.

Acknowledgements

This work has been supported by Spanish Ministry of Science and Innovation through projects MAT 2009-14369-C02-01 and MAT 2006-13480, and Ramón y Cajal fellowship (RYC-2008-03523). Authors thank Dr. M.A.G. Aranda and Dr. L. León-Reina for XRD analyses.

References

[1] D. Taylor, Thermal expansion data XI. Complex oxides, A_2BO_5, and the garnets, Br. Ceram. Trans. J. 86 (1987) 1–6.
[2] D. Taylor, Thermal expansion data. III. Sesquioxides, M_2O_3 with the corundum and the A-, B- and C-M_2O_3 structures, Br. Ceram. Trans. J. 83 (1984) 92–98.
[3] B.R. Lawn, N.P. Padture, L.M. Braun, S.J. Bennison, Model for toughness curves in two-phase ceramics. I. Basic fracture mechanics, J. Am. Ceram. Soc. 76 (1993) 2235–2240.
[4] N.P. Padture, J.L. Runyan, S.J. Bennison, L.M. Braun, B.R. Lawn, Model for toughness curves in two-phase ceramics. II. Microstructural variables, J. Am. Ceram. Soc. 76 (1993) 2241–2247.
[5] N.P. Padture, S.J. Bennison, H.M. Chan, Flaw-tolerance and crack-resistance properties of alumina–aluminium titanate composites with tailored microstructures, J. Am. Ceram. Soc. 76 (1993) 2312–2320.
[6] J.L. Runyan, S.J. Bennison, Fabrication of flaw-tolerant aluminium–titanate-reinforced alumina, J. Eur. Ceram. Soc. 7 (1991) 93–99.
[7] R. Uribe, C. Baudin, Influence of a dispersion of aluminium titanate particles of controlled size on the thermal shock resistance of alumina, J. Am. Ceram. Soc. 86 (2003) 846–850.
[8] C. Baudin, A. Sayir, M.H. Berger, Mechanical behaviour of directionally solidified alumina/aluminium titanate ceramics, Acta Mater. 54 (2006) 3835–3841.
[9] S. Bueno, C. Baudin, Layered materials with high strength and flaw tolerance based on alumina and aluminium titanate, J. Eur. Ceram. Soc. 27 (2007) 1455–1462.
[10] A. Dakskobler, T. Kosmac, Preparation and properties of aluminium titanate–alumina composites, J. Mater. Res. 21 (2006) 448–454.
[11] P. Manurung, I.M. Low, B.H. O'Connor, Effect of beta-spodumene on the phase development in an alumina/aluminium–titanate system, Mater. Res. Bull. 40 (2005) 2047–2055.
[12] S. Bueno, M.H. Berger, R. Moreno, C. Baudín, Fracture behaviour of microcrack free alumina–aluminium titanate ceramics with second phase nanoparticles at alumina grain boundaries, J. Eur. Ceram. Soc. 28 (2008) 1961–1971.
[13] I.D. Alecu, R.J. Stead, Further tailoring of material properties in non-equimolar aluminium titanate ceramic materials, J. Eur. Ceram. Soc. 27 (2007) 679–682.
[14] R. Uribe, Materiales de alúmina/titanato de aluminio con alta resistencia al choque térmico, PhD Thesis, Univ. Autónoma de Madrid (Spain), November 2001.
[15] I.M. Low, Z. Oo, Reformation of phase composition in decomposed aluminium titanate, Mater. Chem. Phys. 111 (2008) 9–12.
[16] A.M. Segadaes, M.R. Morelli, R.G.A. Kiminami, Combustion synthesis of aluminum titanate, J. Eur. Ceram. Soc. 18 (1998) 771–781.

[17] H.A.J. Thomas, R. Stevens, β-Aluminium titanate—a literature review. Part 2. Engineering properties and thermal stability, Br. Ceram. Trans. J. 88 (1989) 184–190.
[18] R.D. Skala, D. Li, I.M. Low, Diffraction, structure and phase stability studies on aluminium titanate, J. Eur. Ceram. Soc. 29 (2009) 67–75.
[19] E. Kato, K. Daimon, J. Takahashi, Decomposition temperature of β-Al_2TiO_5, J. Am. Ceram. Soc. 63 (1980) 355–356.
[20] M. Jayasankar, S. Ananthakumar, P. Mukundan, W. Wunderlich, K.G.K. Warrier, Al_2O_3 @ TiO_2—a simple sol–gel strategy to the synthesis of low temperature sintered alumina–aluminium titanate composites through a core–shell approach, J. Solid State Chem. 181 (2008) 2748–2754.
[21] Y. Yang, Y. Wang, W. Tian, Z. Wang, C. Li, Y. Zhaoa, H. Biana, In situ porous alumina/aluminum titanate ceramic composite prepared by spark plasma sintering from nanostructured powders, Scripta Mater. 60 (2009) 578–581.
[22] I. Santacruz, K. Annapoorani, J. Binner, Preparation of high solids content nano zirconia suspensions, J. Am. Ceram. Soc. 91 (2008) 398–405.
[23] I. Santacruz, C. Baudín, M.I. Nieto, R. Moreno, Improved green strength of ceramics through aqueous gelcasting, Adv. Eng. Mater. 6 (2004) 672–676.
[24] ASTM File 00-021-1272, Database PDF (Power Diffraction File).
[25] ASTM File 01-080-0786, Database PDF (Power Diffraction File).
[26] ASTM File 00-021-1276, Database PDF (Power Diffraction File).
[27] ASTM File 00-026-0040, Database PDF (Power Diffraction File).
[28] S. Bueno, R. Moreno, C. Baudín, Design processing of Al_2O_3–Al_2TiO_5 layered structures, J. Eur. Ceram. Soc. 25 (2005) 847–856.
[29] I. Chen, X.H. Wang, Sintering dense nanocrystalline ceramics without final-stage grain growth, Nature 404 (2000) 168–171.
[30] J. Binner, K. Annapoorani, A. Paul, I. Santacruz, B. Vaidhyanathan, Dense nanostructured zirconia by two stage conventional/hybrid microwave sintering, J. Eur. Ceram. Soc. 28 (2008) 973–977.
[31] S. Bueno, R. Moreno, C. Baudín, Reaction sintered Al_2O_3/Al_2TiO_5 microcrack-free composites obtained by colloidal filtration, J. Eur. Ceram. Soc. 24 (2004) 2785–2791.